DR MIW: Dispersion Relation Magnetoinductive Waveguide Design Tool

C. Jenkins, ***Student Member, IEEE,*** **A. Kiourti,** ***Senior Member, IEEE***

ElectroScience Laboratory, Department of Electrical and Computer Engineering, Ohio State University, Columbus, OH 43212 USA

Manuscript received November 28, 2023; revised April 29, 2024. First published XXXXXX.Current version published XXXXXX. This research was sponsored by the National Science Foundation under NSF Award No. 2053318.

Abstract: Magnetoinductive waveguides (MIWs) consist of a series of electrically small resonant loops used to guide magnetic fields and show high promise for applications in communications, body-area networks, power transfer, and sensing. Design of MIWs typically relies on a multi-step process that involves computationally heavy simulations just to reach an initial, non-optimized geometry. This complexity represents a barrier-to-entry for the expanded use of MIWs. In this work, we introduce a MATLAB-based tool for the synthesis of MIW designs. The tool allows the user to input various geometric or circuit parameters for several types of MIWs (e.g., planar, axial, dual-layer). From these values, electrical characteristics, such as mutual coupling and self-inductance, are estimated and used to calculate the theoretical MIW transmission behavior over frequency. The behavior can then be optimized on-the-fly by adjusting the geometric or circuit parameters. Once the desired performance is achieved, the design parameters can be exported for further use, such as validation in a full-wave simulator. This process offers a significant reduction in design iteration cost in terms of both time and computation, offers increased insight that is not present in single simulation suites, and greatly reduces the obstacles for the expansion of MIW applications.

Index Terms: Electrically small resonant loops, magnetoinductive waveguides, magnetoinductive waves, dispersion diagrams, periodic structures, design tool.

1. Introduction

Magnetoinductive waveguides (MIWs) are a novel technology that have found applications in communications, power transfer and sensing [1]-[4]. They are formed by placing electrically small resonant loops near one another. Current is excited on the transmit loop which, in turn, induces current on the neighboring loops. Careful design leads to a traveling wave phenomenon which has been explored in numerous scenarios, most recently through body-area networks [5]-[7].

Thus far, MIWs have been a fringe technology for a variety of reasons, one of which is the cumbersome design methodology. Specifically, traditional design involves first building a conceptual understanding of MIWs (documented throughout the literature [5]-[10]), and then combining a series of simulations and calculations through the MIW dispersion relation of interest to determine the geometric parameters of the MIW, typically via a tool such as MATLAB [11]-[14]. This can take several hours in just simulation and optimization time alone, not accounting for any errors involved in the process due to lack of familiarity. In both commercial and research environments, this time is expensive and could easily double or triple in length should any design iterations or constraint changes be made.

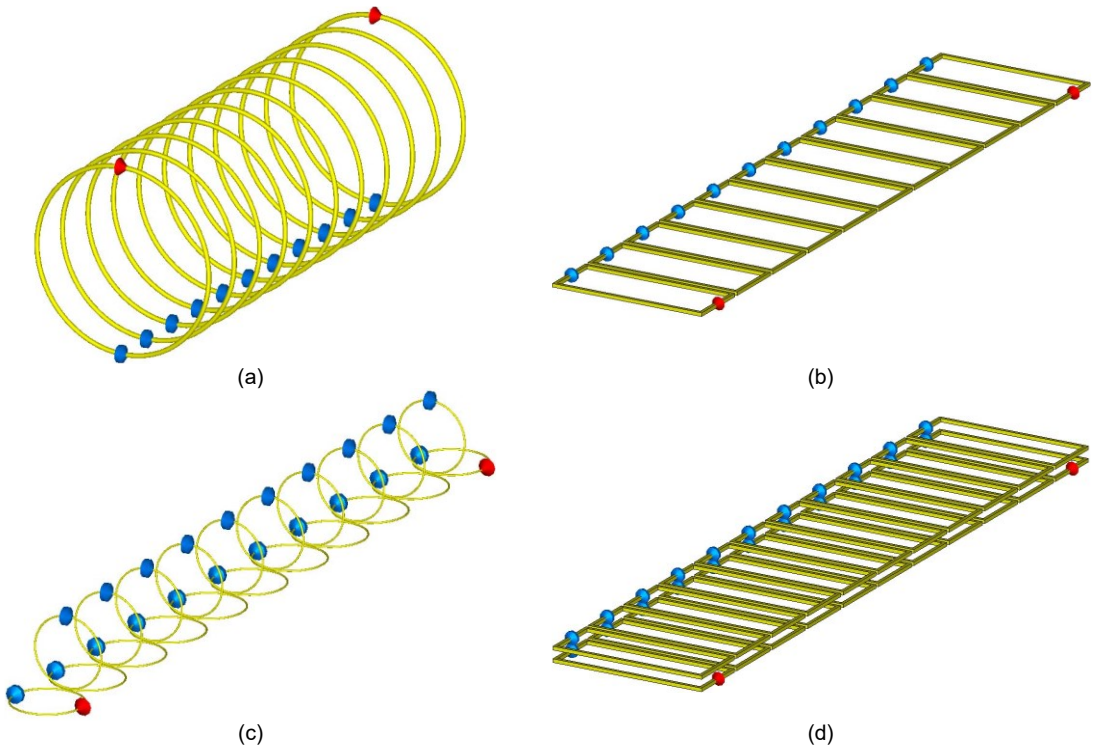

Fig. 1. Relevant MIW geometries of interest: (a) single-loop axial, (b) single-loop planar, (c) axial-planar, and (d) dual-layer planar.

In this work, we introduce a new easy-to-use MATLAB-based tool for MIW design and synthesis [15], namely DR MIW (Dispersion Relation MagnetoInductive Waveguide design tool). DR MIW decreases iteration time by orders of magnitude, with results updating nearly instantly by solving the MIW dispersion relations rather than conducting full geometric simulations. By removing the need to understand the dispersion relations and by including example designs, the amount of working MIW knowledge needed to design the MIW is significantly reduced. Notably, the ability to consider higher-order interactions within the tool means that these benefits are made without compromising the final solution vs. full-wave simulators.

The rest of the manuscript is organized as follows. In Section 2, we describe the analytical model used as the foundation for DR MIW. An overview of the tool follows in Section 3, including a description of various features and approximations that are important to its functionality. Finally, a design example and comparison are presented in Section 4, highlighting the advantages of DR MIW in terms of design time.

2. Analytical Model

For the purposes of the current version of DR MIW, MIWs are broken down into two categories: single-loop element MIWs and dual-loop element MIWs, where the loop number refers to the periodic unit (e.g., two loops form the periodic unit of the dual-loop element MIWs). Within each category, loops can be oriented in two geometric subtypes: axial (i.e., the central axes of the loops are aligned) and planar (i.e., the loops are placed on the same plane). This leads to 5 possible MIW geometries: single-layer axial, single-layer planar, dual-layer axial, axial-planar, and dual-layer planar. The dual-layer axial MIW is not explored in this work, but we note that the dual-loop element theory explored in Section 2.3 remains valid for this case. Fig. 1 shows 3-dimensional (3D) models of the 4 designs of interest, highlighting the capacitor and port locations in blue and red, respectively. We note that a capacitor is needed to make the loops resonant at a desired frequency for proper operation. We also note that the loop shapes shown in Fig. 1 are selected for example purposes only; any loop shape can be used in general.

For ease of analysis, we will walk through the analysis of MIWs constructed through single-loop elements as presented in previous literature which utilizes the well-known impedance matrix method [8]. While the exact equations do not hold for MIWs constructed through dual-loop elements, the process and primary outcomes of the analysis are similar, as discussed in Section 2.3. In this analysis, we also assume that the MIW is infinite in length and each loop is identical. While these are never precisely true, the general behavior is captured very well by the model [5]-[8]. The problem of terminal impedance will be analyzed in Section 2.2, while non-uniform loops are not addressed by the DR MIW tool.

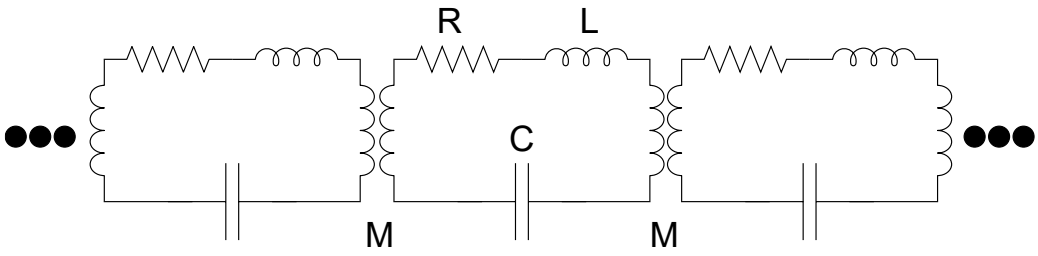

Fig. 2. Circuit model of a general single loop element magnetoinductive waveguide (MIW) for nearest neighbors' interactions only.

The analytical model comes from the analysis of the circuit shown in Fig. 2 which represents a series of tightly-packed lossy resonant loops in either an axial or planar configuration. Here, R is the resistance of the loop, L is the self-inductance, C is the capacitance, and M is the mutual inductance between neighboring loops. For illustrative purposes, we will assume nearest neighbors' interactions only. When using Kirchoff's Voltage Law on the n^{th} loop, we get the following equation:

$$0 = I_n\left(R + j\left(\omega L - \frac{1}{\omega C}\right)\right) + I_{n-1}j\omega M + I_{n+1}j\omega M \tag{1}$$

where ω is the radial frequency. This equation has a non-trivial solution when current is distributed as a traveling wave, namely:

$$I_n = I_0 e^{-n\gamma p} \tag{2}$$

where n indicates the loop number, p represents the physical period of the structure, and $\gamma = \alpha + j\beta$ is the propagation constant (α representing the attenuation and β representing the phase). After some algebraic manipulation, we arrive at the final dispersion relation:

$$-\left(R + j\left(\omega L - \frac{1}{\omega C}\right)\right) = j\omega 2M cosh(\gamma p) \tag{3}$$

This relation holds for any series of electrically small resonant structures, in either an axial or planar configuration, many of which have been previously explored [14], [16]. Clearly, the dispersion relation is highly dependent on the geometry of the MIW, both in the loop shape (L and R) and the space between loops (M). For the scope of the tool, geometric calculations are limited to circular and rectangular loops.

2.1. Propagation Constant

The primary output of Eq. (3) is the propagation constant, $\gamma = \alpha + j\beta$. The attenuation constant, α, is measured in Np/m and represents the loss of the waveguide. Traditionally, in MIW analysis, αp is plotted which represents the loss per loop. This is done to normalize results against any transmission distance for ease of comparison. Total loss is then $N\alpha p$ where N is the total number of loops. An example attenuation constant plot is shown in Fig. 3(a). The overall shape of the attenuation constant curve is very typical for an MIW, with a clear passband centered around the resonant frequency of the loops.

The phase constant, β, is also measured in Np/m and defines the theoretical operating frequencies of the MIW. For any β in the range $0 < \beta < \pi$, the propagation constant has an imaginary component which indicates propagation along the MIW. When $\beta = 0$ or π, the propagation constant is entirely real, leading to an exponential decay. These values can be solved for directly, leading to a bandwidth defined by the following expression for a single-loop MIW [17]:

$$\sqrt{\frac{1}{LC\left(1 + \left|\frac{2M}{L}\right|\right)}} < \omega < \sqrt{\frac{1}{LC\left(1 - \left|\frac{2M}{L}\right|\right)}} \tag{4}$$

An example phase constant plot is shown in Fig. 3(b). Note that the slope of the line is directly related to the sign of the mutual inductance between the loops.

2.2. Terminal Impedance

Due to the traveling wave nature of MIW propagation, a finite MIW must be loaded with an additional terminal impedance to avoid reflections at the ports. This is like the termination needed in a traditional transmission line, where matching techniques are used to reduce reflections at the ports. The derivation of the required terminal impedance for single-loop element MIWs follows from voltage analysis of a terminal loop, which only has coupled neighbors in one direction. To match the impedance, we need to terminate the loop with an impedance equal to

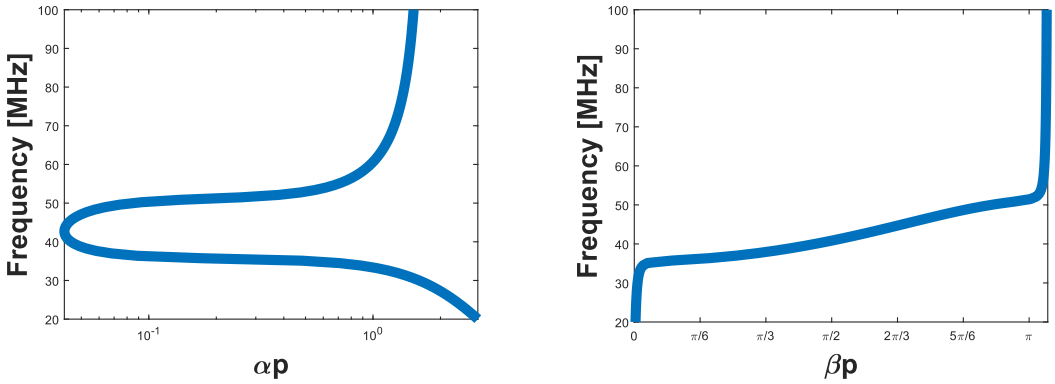

Fig. 3. Example propagation constant graphs, (a) attenuation constant vs frequency and, (b) phase constant vs frequency

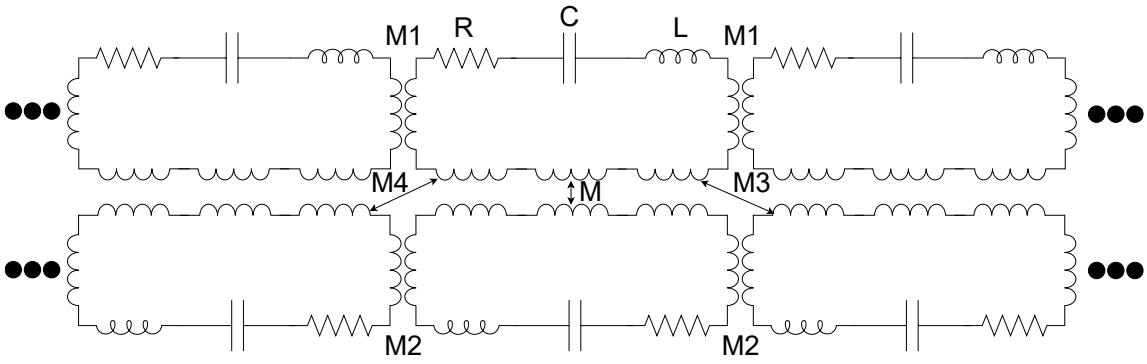

Fig. 4. Circuit model of a dual loop element magnetoinductive waveguide (MIW) for nearest neighbors' interactions only.

that of the excepted coupled neighbors. When considering only nearest neighbor coupling, the terminal impedance is defined as:

$$Z_t = j\omega M e^{-\gamma p} \tag{5}$$

This impedance is purely real at the resonant frequency of the loops but is complex for all other frequencies [8]. When higher-order coupling is considered, this impedance is complex in general.

2.3. Dual-Loop Element MIWs

Dual-loop element MIWs have an equivalent circuit model shown in Fig. 4. This circuit model and the accompanying analysis is valid for both dual-layer planar and axial-planar MIWs. While the geometry complexity is increased significantly compared to the single-layer model of Fig. 2, the circuit analysis does not change and has been explored in literature [9]. Following the same procedure, the dispersion relation for dual-loop element MIWs is:

$$\begin{aligned}&\left(Z + 2j\omega M_1 \cosh(\gamma p)\right)\left(Z + 2j\omega M_2 \cosh(\gamma p)\right)\\ &= -\omega^2(M^2 + M_3^2 + M_4^2 + 2M(M_3 + M_4)\cosh(\gamma p) + 2M_3 M_4 \cosh(2\gamma p))\end{aligned} \tag{6}$$

From here, both the bandwidth and terminal impedance can likewise be extracted using the same process as above. Note that the quadratic nature of the dispersion relation leads to two possible propagation constants under specific geometric configurations.

3. DR MIW Tool

The two presented dispersion relations (Eq. (3) and Eq. (6)) are the foundation for MIW design. The DR MIW tool is built upon solving these dispersion relations under any geometric configuration or using any equivalent circuit parameters to estimate the performance of an MIW with a high degree of accuracy. Specifically, the DR MIW tool is a MATLAB App that requires access to the Signal Processing Toolbox, Symbolic Math Toolbox, and the latest version of MATLAB (R2023b at the time of writing) to properly make changes to the code. To run the application without MATLAB, the R2023b MATLAB Runtime Compiler is needed along with the .exe version of the tool.

On **Startup**, the user is provided with the available options, as shown in Fig. 5. The image and parameter fields dynamically change depending on the selected **MIW Type** (axial, planar, dual-layer planar, and axial-planar),

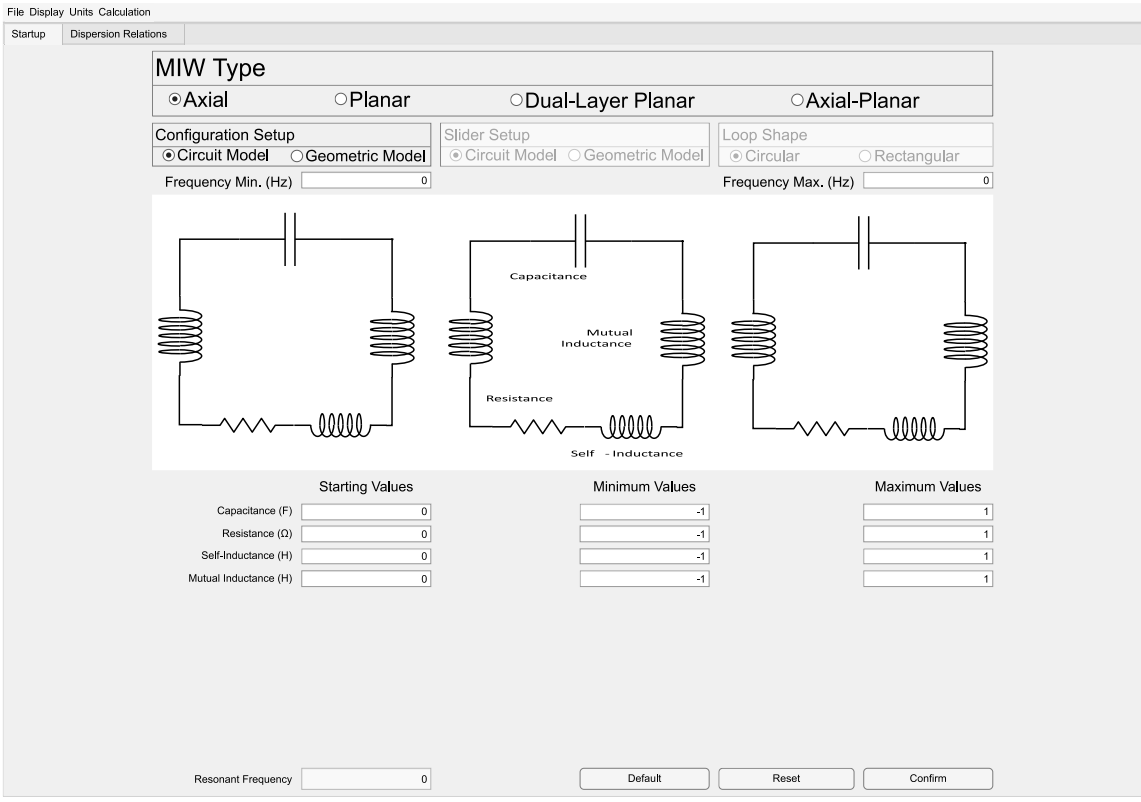

Fig. 5. DR MIW Tool on initial startup.

Configuration Setup (circuit model or geometric model, as will be discussed in detail in Sections 3.1 and 3.2, respectively), **Slider Setup** (circuit model or geometric model) and selected **Loop Shape** (circular or rectangular). For each possible configuration, pressing the **Default** button will automatically fill out the parameter fields corresponding to an example MIW design. Pressing the **Reset** button will return the program to the startup state. When a value is entered into the Starting Values field, the minimum and maximum values are automatically calculated, but can be changed by the user without error.

Once the necessary parameters are inserted, the **Resonant Frequency** field will automatically update based on the **Capacitance** and **Self-Inductance** of the selected model and the typical resonance definition ($f_0 = 1/2\pi\sqrt{LC}$). Since the resonant frequency of the structure is very important to MIW function, this field can be used to adjust values until the desired resonance is achieved without requiring a full solution of the dispersion relation. Once the **Confirm** button is pressed, a series of calculations will occur in the background depending on the configuration setup, as described in Sections 3.1 and 3.2, to determine the equivalent circuit model parameters. From here, the dispersion relation of interest (Eq. (3) and Eq. (6)) is solved either analytically (first order coupling only) or numerically (higher-order coupling) for the propagation constant.

When the solution is complete, the tab will automatically switch to the **Dispersion Relations** tab. If any error is present in the setup, the tab will not be switched and instead an error message will display. Note that pressing the **Confirm** button is the only time the two tabs interact with one another, and will overwrite any active design in the **Dispersion Relations** tab. If the button is not pressed, no changes made in the **Startup** tab will affect the **Dispersion Relations** tab.

The **Dispersion Relations** tab for an example MIW is shown in Fig. 6. Four figures are generated showing the real and imaginary parts of the propagation constant and terminal impedance across frequency. Five text areas are also filled with important specifications related to the current design: minimum loss, bandwidth, resonant frequency, terminal impedance, and solution order used. These specification fields can be removed by accessing the **Display** tool bar and deselecting the field(s) of concern. The units used in the figures and in the specification fields can be changed in the **Units** tool bar. Specifically, the frequency can be listed in Hz, MHz, GHz and as a fraction of the resonant frequency and the loss can be listed in linear or log scale. In the **Calculation** tool bar, the bandwidth calculation can be switched between a theoretical limit as determined by the first-order dispersion relation or by a change from the minimum loss. In the same menu, the terminal impedance can either be listed at the resonant frequency or at the frequency of minimum loss. Here we note that while it is technically possible to

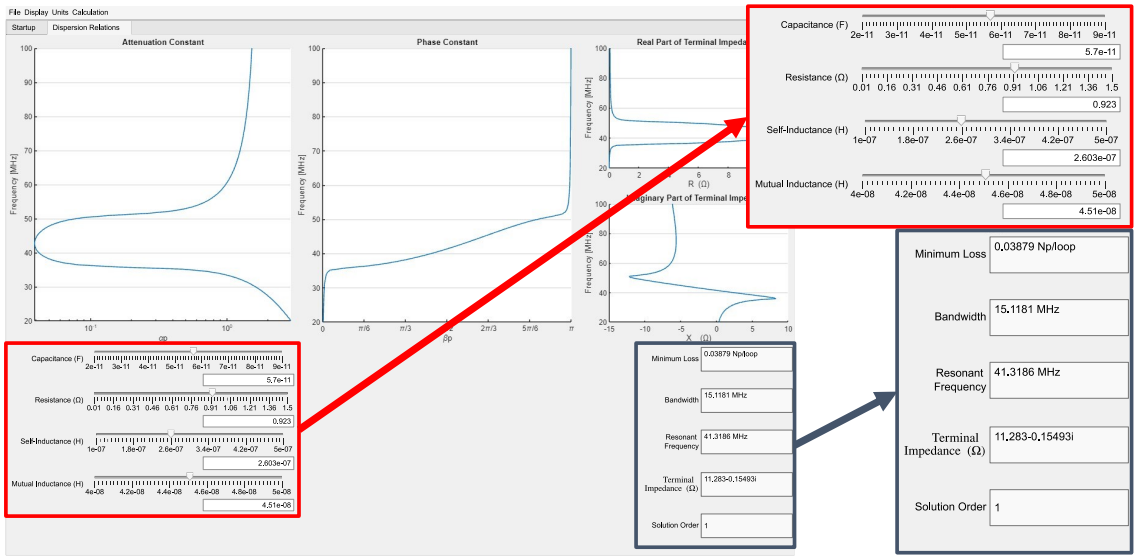

Fig. 6. Dispersion Relations tab for example single-loop element. Circuit model-based MIW with slider and specification fields highlighted.

extract the equivalent circuit parameters necessary to achieve a specific resonance, bandwidth, and minimum attenuation for a single-loop element MIW, we have not implemented this reverse design process within the tool. This is only possible for the single-loop element case with the circuit model-based approach. As such, implementation of the reverse design process would fracture the cohesiveness of the tool, while simultaneously obfuscating the relationship between circuit parameters and geometry.

Each parameter from the **Startup** tab has a corresponding slider and field on the **Dispersion Relation** tab. Adjusting any slider leads to the generation of a new solution and an update of the figures and specification fields. Entering in a new value into one of the parameter fields will have the same effect, but it will also cause the limits of the corresponding slider to change such that the new value is the center value of the slider.

At any point while using the DR MIW Tool, the state of the app can be saved by accessing the **Save As** button under the **File** toolbar. The state will be saved as a .mat file which can then be loaded at any time by pressing the Open button under the File toolbar and selecting the appropriate file in the pop-up window. If the **Save As** button has been used or if a file has been opened, the **Save** button will overwrite the file with the new state of the application if pressed.

While the process is the same regardless of the input options selected, the behind-the-scenes calculations change significantly. In particular, the changes between the circuit model and geometric model configurations are drastic in terms of computational complexity and baseline assumptions. As such it is important to understand each one to determine which model is appropriate for each specific use-case.

3.1 Circuit Model Configuration Setup

The **Circuit Model** configuration setup allows the user to directly input the equivalent circuit parameters of the MIW (e.g., resistance, mutual inductance, etc.). This implementation is particularly useful for the design of non-loop based MIWs as the dispersion relations are generalizable to arbitrary shapes so long as the circuit parameters are accurate, and the shape is electrically small. To reduce complexity of user interaction, the current **Circuit Model** configuration is limited to first-order solutions as any higher orders would require direct input of many more mutual inductance values. This reduction in complexity also allows the solution to be solved analytically in both the single-loop and dual-loop element MIW designs, drastically decreasing computational load and iteration time. As such, this model is also suitable for experienced designers who have a strong understanding of how changes in equivalent circuit parameter values correspond to changes in geometry. Additionally, because the geometry is not considered in this mode, selecting the **Axial** MIW type will yield the same solution as selecting the **Planar** MIW type and likewise with the **Dual-Layer Planar** MIW type and **Axial-Planar** MIW type since each pair has the same dispersion relation, as discussed in Section 2.

3.2. Geometric Model Configuration Setup

The **Geometric Model** configuration setup is significantly more complex than the **Circuit Model**. Before the dispersion relation can be solved, the equivalent circuit parameters must first be estimated based on the entered geometry. The three parameters of interest are: resistance, self-inductance, and mutual inductance. For

resistance, a cylindrical wire model is used and effects such as skin depth are ignored leading to a resistance equation equal to:

$$\mathrm{R} = \frac{C}{\sigma \mathrm{A}} \tag{7}$$

where R is the resistance in ohms, C is the circumference of the loop, σ is the conductivity in S/m and A is the cross-sectional area of the cylindrical wire in square meters. For self-inductance, the general equation is dependent on the exact geometry of the current carrying wire. By limiting the geometric model to rectangular and circular loops, the self-inductance can be approximated.

The selected model for circular loops assumes a uniform shape and thick wire, leading to the well-known approximation [18]

$$\mathrm{L_{circ}} = \mu_0 r_1 \left(\ln\left(\frac{8r_1}{r_2}\right) - 2 \right) \tag{8}$$

where μ_0 is free space permeability, r_1 is the radius of the loop, and r_2 is the wire radius.

For rectangular loops, another common model is used that assumes a uniform rectangular loop and thick wire with l as the length of the loop and w as the width [19]:

$$\begin{aligned} \mathrm{L}_{rect} = \frac{\mu_0}{\pi}\Bigg(& -2(l+w) + 2\sqrt{l^2+w^2} - l\ln\left(\frac{l+\sqrt{l^2+w^2}}{w}\right) \\ & - w\ln\left(\frac{w+\sqrt{l^2+w^2}}{l}\right) + l\ln\left(\frac{2l}{r_2}\right) + w\ln\left(\frac{2w}{r_2}\right)\Bigg) \end{aligned} \tag{9}$$

In general, mutual inductance depends on the shape of the two objects, their orientation, and the 3D spacing between them. This is a highly complex problem to solve in general. As such, we again look for appropriate approximations for the coupling between two circular loops and the coupling between two rectangular loops. The model in [20] is used for circular loops and assumes filamentary wire, single turn, and identical radius loops with their axes aligned. By doing so, the mutual inductance can be calculated as:

$$M_{circ} = \frac{\mu_0}{4\pi}\int_0^{2\pi}\int_0^{2\pi} \frac{r_1^2(\sin(\theta)\sin(\varphi) + \cos(\alpha)\cos(\theta)\cos(\varphi))\, d\theta\, d\varphi}{\sqrt{(r_1\cos(\theta) - r_1\cos(\varphi))^2 + (r_1\sin(\theta) - r_1\sin(\varphi)\cos(\alpha) - c)^2 + (r_1\sin(\varphi)\sin(\alpha) - d)^2}} \tag{10}$$

where α is the angular misalignment between the loops, d is the vertical separation between the loops, and c is the transverse misalignment between the loop centers. For the coupling between two rectangular loops, the model in [21] is used instead, which assumes identical filamentary loops with their axes aligned. In this case, the mutual inductance can be calculated as:

$$M_{rect} = \frac{2\mu_0}{\pi^2}\iint_{-\infty}^{\infty} \sqrt{a^2+b^2}\, e^{-z\sqrt{a^2+b^2}+j(ax+by)} \left(\frac{\sin(0.5al)}{a}\frac{\sin(0.5bw)}{b}\right)^2 da\, db \tag{11}$$

where z is the vertical separation between the loops, and x and y are the transverse and longitudinal misalignment respectively.

Many of these calculations, particularly those for mutual inductance, can take much longer to complete than the **Circuit Model** configuration. As such, the **Geometric Model** is always slower than the **Circuit Model**, and greater complexity in geometry leaves to longer computation times (e.g., a geometric dual-layer planar MIW solution would take longer to calculate than a geometric axial MIW). Even with this limitation, the time scale to reach the solution is in minutes rather than hours for a full-wave simulation with complex geometry.

3.2.1. Higher-Order Coupling

Because of the input limitations mentioned in Section 3.1, higher-order coupling is only available for **Geometric Model** inputs. Looking at the general dispersion relation for single-loop element MIWs for any order coupling, we see:

$$-\left(R + j\left(\omega L - \frac{1}{\omega C}\right)\right) = j\omega 2\sum_{u=1}^{N} M_u \cosh(u\gamma p) \tag{12}$$

which cannot be solved analytically without first selecting a value for N. As such, for higher-order coupling solutions, the tool solves these numerically using built in MATLAB functions. These solutions can be unstable and lead to spurious results, particularly as N increases because of the potential for multiple solutions. A strange result of the numerical solution is that even values of N cannot be used as the results are severely incorrect. These same errors become more pronounced for the dual-loop element MIWs. A solution to controlling this error has not been found for these MIWs. As such, higher-order coupling is not currently implemented for dual-loop element MIWs.

To reach a higher-order solution for the single-loop element MIWs, the first-order solution is first solved for analytically. Then, N mutual inductance values are calculated. N can either be set exactly by the user or can be

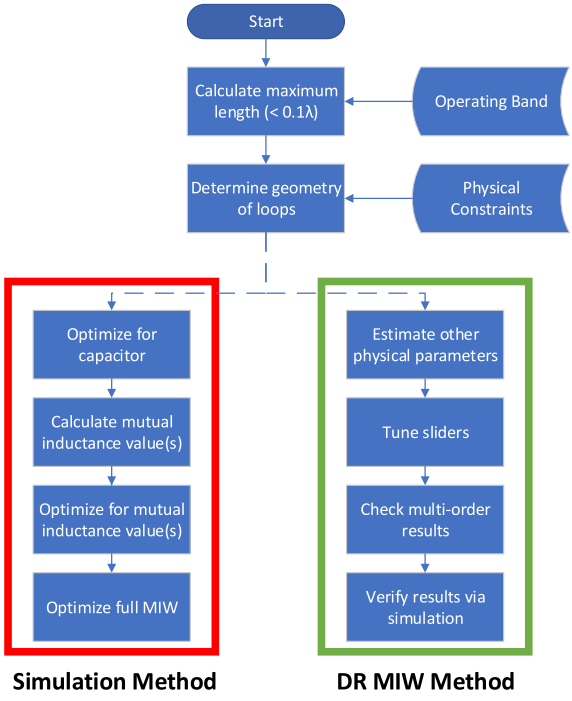

Fig. 7. Process comparison between simulation and DR MIW Tool for a general MIW design.

determined based on the percent change of the mutual inductance values from the initial first-order value and a user-defined threshold. The mutual inductance values are then used to create a symbolic expression in terms of the propagation constant according to the multi-order dispersion relation. The propagation constant is then solved for numerically, using the first-order analytic solution as an initial guess to speed up the solver.

Because several mutual inductance values must be calculated, and then a potentially complex symbolic expression must be solved numerically, higher-order solutions take significantly longer to reach than first-order solutions. As such, it is not recommended to use the higher-order solution mode throughout the entire design process. Instead, use the first-order solution to reach a strong starting point and then use the higher-order solutions to make any additional small adjustments.

4. Design Examples

A comparison of the simulation and DR MIW process for electrically small resonant loop MIWs is described in Fig. 7. Both processes share initial common steps based on the physical constraints of the loops, after which they are split. For the simulation path, a minimum of three simulation models are needed and each model could be run many times for optimization purposes. Even for a simple design that requires little optimization, the length of this process is on the scale of hours. Alternatively, the DR MIW process requires no simulations except in the case when verification is necessary. For any design, the length of the process is on the scale of minutes, especially if higher-order interactions are minimal.

To compare the design process, we explore a sample scenario. The goal is to design an axial MIW for integration into a Bluetooth system using 30 American Wire Gauge (AWG) rectangular copper loops. This requires operation from 2.4 to 2.48 GHz. The center frequency of 2.44 GHz limits the circumference of the loops to a maximum of 1.23 cm ($< 0.1\lambda$). According to known best practices [6], the ratio from length to width are determined with length being set at 0.17 cm and width being set at 0.44 cm. From here, the process paths split.

4.2. Full-wave simulation

For the simulation method, the finite-element method, frequency domain solver in CST Studio [22] is used with the default adaptive meshing algorithm based on an S-Parameter convergence of 0.02. For optimization, CST's Trust Region Framework algorithm is employed using the squared difference goal normalization and domain accuracy of 0.01. This setup has successfully shown agreement with experimental results in other similar designs [5], [6], [7]. First, a single loop is modeled and simulated to determine the capacitor value. The capacitor is then included in the model and the capacitance value is optimized through 5 iterations to 0.92 pF. Next, Eq. (4) is used to determine that the mutual inductance value must be at least 75 pH to achieve the proper bandwidth. An optimization is then conducted on the gap size between two coplanar loops to reach the desired mutual

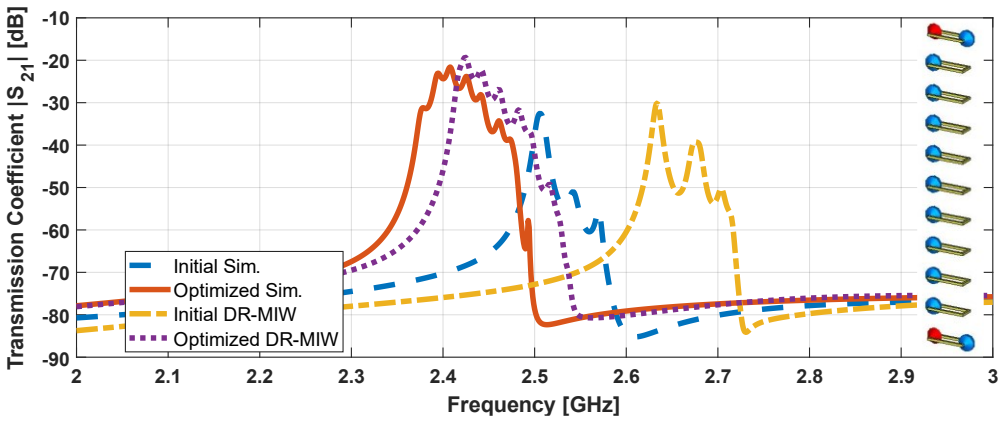

Fig. 8. Transmission coefficient ($|S_{21}|$) results with the relevant design geometry inserted.

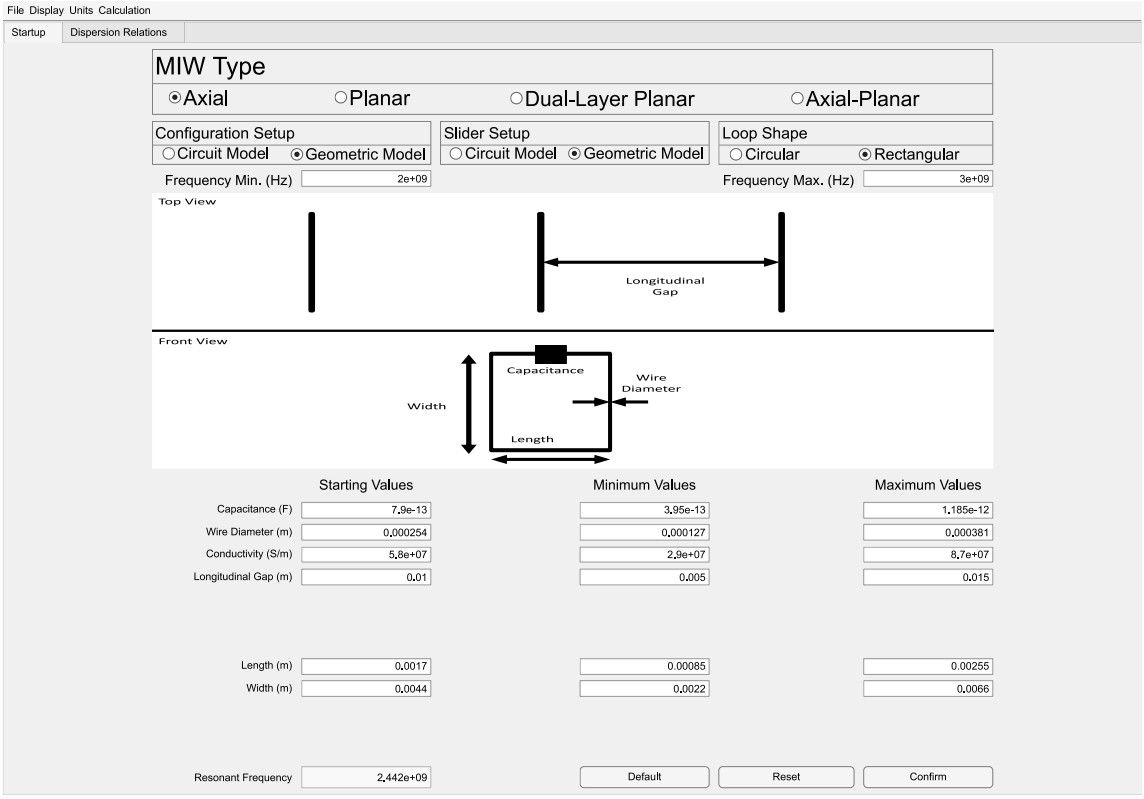

Fig. 9. DR MIW Tool **Startup** tab for design example

inductance value with a gap of 0.383 cm through 5 iterations. Finally, an 11-loop MIW is modeled and optimized to achieve a clear passband covering 2.4 to 2.48 GHz. With the initial parameters, the MIW achieves a passband extending from 2.47 GHz to 2.52 GHz. After optimizing the capacitor value to 0.99 pF and gap between loops to 0.354 cm, the passband reaches the desired 2.4 to 2.48 GHz through 11 iterations. The initial and optimized transmission results ($|S_{21}|$) are shown in Fig. 8 along with a model of the MIW geometry.

4.3. DR MIW Process

Using the DR MIW Tool, the **MIW Design** is selected as axial, the **Configuration Setup** and **Slider Setup** as geometric, and the **Loop Shape** as rectangular. Next, the known quantities are inserted into the parameter fields (wire diameter, conductivity, length, and width). On the **Startup** tab, the capacitor value is changed until the resonant frequency field is approximately 2.44 GHz, leading to a value of 0.79 pF. For the gap size, an initial guess of 0.1 cm is selected such that the gap size is on the scale of the loop size. The completed **Startup** tab is shown in Fig. 9. By adjusting the sliders on the Dispersion Relations tab, a 0.4 cm gap is found to achieve the appropriate 80 MHz bandwidth centered at 2.44 GHz. The solution order is then set to 5 to verify the performance

with higher-order coupling. To verify the results, the MIW is modeled in CST Studio, showing a slight frequency shift in the passband to 2.65 GHz. After optimizing the capacitor value to 0.94 pF and gap to 0.35 cm through 14 iterations, the desired passband is achieved as shown in Fig. 8.

4.4. Comparison

As expected, both procedures reached the desired performance despite the very different approaches. To compare the efficiency of the approaches, each step was timed, as shown in Table I. The DR MIW Tool was used on a consumer grade laptop (16 GB RAM, Intel i7-1165G7 processor) while the simulations were run on a high-performance server (256 GB RAM, Intel Xeon E5-2680 v4 processor). Despite the significant decrease in computational power, the DR MIW method is 3.75 times faster than the simulation method when including the final design optimization. The need for the final design optimization for the DR MIW method is highly dependent on the design itself, and as such is not always required. The same cannot be said for the simulation method. With this in mind, the time savings of the DR MIW method could potentially be expanded to as much as 22.5 times faster than the simulation method. Regardless, the DR MIW tool significantly speeds up the MIW design process leading to significant time savings.

TABLE I
MIW Design Process Comparison

Step	Simulation Method	DR MIW Method
Capacitor Optimization	0.25 hours	1 minute
Gap Optimization	1 hour	5 minutes
Final Design Optimization	1 hour	30 minutes
Total Time:	2.25 hours	36 minutes

5. Conclusions

We have demonstrated a dispersion relation MIW design tool that is completely open-source and free to access. This tool can speed up the MIW design process by orders of magnitude without sacrificing accuracy, removing a significant barrier to entry for the accessibility of MIWs. Despite this, the tool does have some limitations due to the numerical approximations used during calculations, instability of results when relying on numerical solvers and lack of consideration of phenomenon such as capacitive coupling or radiative losses. As such, this tool is not recommended for edge case designs that require special attention to these effects (i.e., elements are no longer electrically small, or elements must be placed extremely close together). By making the tool in MATLAB and making the code open source, we hope that the tool can be expanded significantly. Suggested future work on the tool includes implementing a reverse-design process where circuit parameters are calculated from desired performance, adding an integrated design optimizer, improving the application of higher-order coupling, implementing other relevant conductor shapes, including the impact of advanced effects such as retardation into the results, implementing a method of designing multi-dimensional MIW arrays, and implementing a transducer-MIW co-design process.

References

[1] C. Jenkins and A. Kiourti, “Low-Loss Wireless Implant Telemetry Using Magnetoinductive Waveguides,” in *2023 International Applied Computational Electromagnetics Society Symposium (ACES)*, Mar. 2023, pp. 1–2. doi: 10.23919/ACES57841.2023.10114778.

[2] C. J. Stevens, C. W. T. Chan, K. Stamatis, and D. J. Edwards, “Magnetic Metamaterials as 1-D Data Transfer Channels: An Application for Magneto-Inductive Waves,” *IEEE Trans. Microwave Theory Techn.*, vol. 58, no. 5, pp. 1248–1256, May 2010, doi: 10.1109/TMTT.2010.2045562.

[3] J. Yan, C. J. Stevens, and E. Shamonina, “A Metamaterial Position Sensor Based on Magnetoinductive Waves,” *IEEE Open J. Antennas Propag.*, vol. 2, pp. 259–268, 2021, doi: 10.1109/OJAP.2021.3057135.

[4] C. J. Stevens, “Magnetoinductive Waves and Wireless Power Transfer,” *IEEE Trans. Power Electron.*, vol. 30, no. 11, pp. 6182–6190, Nov. 2015, doi: 10.1109/TPEL.2014.2369811.

[5] C. B. Jenkins and A. Kiourti, “Wearable Dual-Layer Planar Magnetoinductive Waveguide for Wireless Body Area Networks,” *IEEE Transactions on Antennas and Propagation*, vol. 71, no. 8, pp. 6893–6905, Aug. 2023, doi: 10.1109/TAP.2023.3286042.

[6] V. Mishra and A. Kiourti, “Wearable Planar Magnetoinductive Waveguide: A Low-Loss Approach to WBANs,” *IEEE Trans. Antennas Propagat.*, vol. 69, no. 11, pp. 7278–7289, Nov. 2021, doi: 10.1109/TAP.2021.3070681.

[7] V. Mishra and A. Kiourti, “Wearable Magnetoinductive Waveguide for Low-Loss Wireless Body Area Networks,” *IEEE Trans. Antennas Propagat.*, vol. 69, no. 5, pp. 2864–2876, May 2021, doi: 10.1109/TAP.2020.3030987.

[8] E. Shamonina, V. A. Kalinin, K. H. Ringhofer, and L. Solymar, “Magnetoinductive waves in one, two, and three dimensions,” *Journal of Applied Physics*, vol. 92, no. 10, pp. 6252–6261, Nov. 2002, doi: 10.1063/1.1510945.

[9] O. Sydoruk *et al.*, “Tailoring the near-field guiding properties of magnetic metamaterials with two resonant elements per unit cell,” *Phys. Rev. B*, vol. 73, no. 22, p. 224406, Jun. 2006, doi: 10.1103/PhysRevB.73.224406.

[10] L. Solymar and E. Shamonina, *Waves in metamaterials*. Oxford ; New York: Oxford University Press, 2009.

[11] K. Segkhoonthod, R. R. A. Syms, and I. R. Young, “Design of Magneto-Inductive Magnetic Resonance Imaging Catheters,” *IEEE Sensors J.*, vol. 14, no. 5, pp. 1505–1513, May 2014, doi: 10.1109/JSEN.2013.2296852.
[12] A. Radkovskaya *et al.*, “An experimental study of the properties of magnetoinductive waves in the presence of retardation,” *Journal of Magnetism and Magnetic Materials*, vol. 300, no. 1, pp. 29–32, May 2006, doi: 10.1016/j.jmmm.2005.10.026.
[13] Zhi Sun and I. F. Akyildiz, “Magnetic Induction Communications for Wireless Underground Sensor Networks,” *IEEE Trans. Antennas Propagat.*, vol. 58, no. 7, pp. 2426–2435, Jul. 2010, doi: 10.1109/TAP.2010.2048858.
[14] A. Hajiaghajani, A. H. Afandizadeh Zargari, M. Dautta, A. Jimenez, F. Kurdahi, and P. Tseng, “Textile-integrated metamaterials for near-field multibody area networks,” *Nat Electron*, vol. 4, no. 11, Art. no. 11, Nov. 2021, doi: 10.1038/s41928-021-00663-0.
[15] “MathWorks - Makers of MATLAB and Simulink.” Accessed: Nov. 08, 2023. [Online]. Available: https://www.mathworks.com/
[16] R. R. A. Syms, L. Solymar, I. R. Young, and T. Floume, “Thin-film magneto-inductive cables,” *J. Phys. D: Appl. Phys.*, vol. 43, no. 5, p. 055102, Feb. 2010, doi: 10.1088/0022-3727/43/5/055102.
[17] E. Shamonina and L. Solymar, “Magneto-inductive waves supported by metamaterial elements: components for a one-dimensional waveguide,” *J. Phys. D: Appl. Phys.*, vol. 37, no. 3, pp. 362–367, Feb. 2004, doi: 10.1088/0022-3727/37/3/008.
[18] E. Bogatin, “Estimating wire & loop inductance: Rule of Thumb #15,” EDN. Accessed: Nov. 08, 2023. [Online]. Available: https://www.edn.com/estimating-wire-loop-inductance-rule-of-thumb-15/
[19] “Rectangle Loop Inductance Calculator - Engineering Calculators & Tools.” Accessed: Nov. 08, 2023. [Online]. Available: https://www.allaboutcircuits.com/tools/rectangle-loop-inductance-calculator/
[20] X. Zhang, H. Meng, B. Wei, S. Wang, and Q. Yang, “Mutual inductance calculation for coils with misalignment in wireless power transfer,” *J. eng.*, vol. 2019, no. 16, pp. 1041–1044, Mar. 2019, doi: 10.1049/joe.2018.8670.
[21] W. Dehui, H. Chao, Y. Fan, and S. Qisheng, “Analytical calculations of self- and mutual inductances for rectangular coils with lateral misalignment in IPT,” *IET Power Electronics*, vol. 12, no. 15, pp. 4054–4062, 2019, doi: 10.1049/iet-pel.2019.0821.
[22] Dassault Systemes, “Electromagnetic Simulation Solvers | CST Studio Suite,” Dassault Systemes. Accessed: Sep. 07, 2023. [Online]. Available: https://www.3ds.com/products-services/simulia/products/cst-studio-suite/solvers/